

A Data-driven Approach to Multi-event Analytics in Large-scale Power Systems Using Factor Model

Fan Yang, Xing He, Robert Caiming Qiu, *Fellow, IEEE* and Zenan Ling

Abstract—Multi-event detection and recognition in real time is of challenge for a modern grid as its feature is usually non-identifiable. Based on factor model, this paper proposes a data-driven method as an alternative solution under the framework of random matrix theory. This method maps the raw data into a high-dimensional space with two parts: 1) the principal components (factors, mapping event signals); and 2) time series residuals (bulk, mapping white/non-Gaussian noises). The spatial information is extracted from factors, and the temporal information from residuals. Taking both spatial-temporal correlation into account, this method is able to reveal the multi-event: its components and their respective details, e.g., occurring time. Case studies based on the standard IEEE 118-bus system validate the proposed method.

Index Terms—multiple event analytics; factor model; power systems; spatial-temporal correlation; time series; random matrix;

I. INTRODUCTION

FOR a large-scale power system, multiple events can hardly be identified properly as it is difficult to distinguish the features of multi-event from the ones of single-event. The multi-event poses a more serious threat to the systems: it can hardly be identified, and thus be addressed, which may lead to a wide-spread blackout.

This paper proposes a statistical, data-driven solution, rather than its deterministic, empirical or model-based counterpart, to solve the problem given above. The study is built upon our previous work in the last several years. See Section I-B for details.

A. Contribution

This paper, based on random matrix theory (RMT), proposes a high statistical tool, namely, factor model, for multi-event detection and recognition in a modern grid. This paper extracts the spatial and temporal information from the massive raw data, respectively, in the form of principal components (factors) and residuals (bulk). The factors map event signals, and the residuals map white/non-Gaussian noises.

The proposed method can be used for multi-event analytics effectively. To the factors, we experimentally obtain that there is a linear relationship between the number of factors and the event number of the multi-event. To the residuals, on the other hand, we extract their information rather than simply assuming it to be identically independent pure white noise as [1]. Time series information contained in noise, together with the spatial information in factors, reveals the multi-event status. The proposed method is practical for real-time analysis.

Besides, the proposed solution is model-free, requiring no knowledge of topologies or parameters of the power system [2–4], and able to handle non-Gaussian noises. To the best of our knowledge, it is the first time to propose an algorithm aiming at multi-event detection based on random matrix theory in the field of power systems.

B. Related Work

In our previous work, a universal architecture with big data analytics is proposed [5] and is applied for anomaly detection [6, 7]. Little work, however, has been done to multi-event analytics in a complex situation. Current researches on event analysis are mainly model-based, aiming at single-event analytics. They may not be suitable for real-time analytics in a complex situation [8]. Some other methods adopt graph theory [9, 10]; the methods strongly depend on the structure of the power system.

Some data-driven methods for event analysis are proposed recently [11] and applied for multi-event analytics [12].

Rafferty utilizes principal component analysis (PCA) for real-time multi-event detection and classification in [12]. In his approach, a threshold of cumulative percentage of total variation is selected in advance. Then, the number of principal components is determined according to the threshold mentioned above. The threshold is selected empirically and subjectively. Besides, for other supervised tools, like deep learning [13] and kernel-based algorithms [14], which are hot-spot to data-driven approaches, the same problem is inevitable. The deep learning algorithms automatically select the features from the massive datasets. This is one big advantage of deep learning over our paradigm. Our paradigm, however, has the advantage of transparency in that our results are provably. Also, our paradigm is deeply rooted in random matrix theory.

Nowadays, high-dimensional factor model has been actively studied and already successfully applied in statistics [15], econometrics [16] and biology [17].

II. THEORY FOUNDATION AND DATA PROCESSING

The frequently used notations are given in Table 1.

A. Random Matrix Theory and Spectral Analytics

Random matrices have been an important issue in multivariate statistical analysis since the landmark work of Wigner and Wishart [18], motivated by problems in quantum physics. Factor model, on the other side, can be used to identify non-random properties (in the form of spikes/outliers) which are

deviations from the universal predictions (in the form of bulk) [19, 20]. To be specific, the eigenvalues of covariance matrix (spectrum) can usually be divided into two parts: a bulk and several spikes. The bulk represents the noises, while the spikes represent the signals, namely, factors.

In previous work, noises are usually assumed to be identically independent in power systems, namely, white noises. However, "no information" or "pure noise" assumption is invalid in practice. For instance, for a certain PMU, there exists time correlation between the measured voltage magnitude data of adjacent sampling points [21, 22]. The time correlation is non-ignorable, especially for a large inter-connected system! This paper formulates the noises using time series analytics.

TABLE I: Some Frequently Used Notations

Notations	Means
$\mathbf{X}, \mathbf{x}, x_{i,j}$	a matrix, a vector, an entry of a matrix
$\mu(x), \sigma(x)$	mean, variance for x
Ω	raw data source
$\mathbb{C}^{N \times T}$	$N \times T$ dimensional complex space
N, T	the row and column size of moving split-window
n	the number of measurable status variables
t_i	the sampling time
$\tilde{\mathbf{X}}$	a raw data matrix
$\tilde{\mathbf{X}}$	a standard non-Hermitian matrix
p	the number of factors
b	the covariance structure of residuals
z	a complex eigenvalue, $z = \lambda + i\varepsilon$
$\hat{p}, \hat{\theta}$	the estimated value of p, θ

Reference [23] provides a fundamental theory to estimate noises, and formulates them as:

$$\mathbf{U} = \mathbf{A}_N^{1/2} \mathbf{G} \mathbf{B}_T^{1/2} \quad (1)$$

where \mathbf{G} is an $N \times T$ matrix with i.i.d (identically independent distribution) Gaussian entries, and \mathbf{A}_N and \mathbf{B}_T are $N \times N$ and $T \times T$ symmetric non-negative definite matrices, representing cross- and auto- covariances, respectively. For more details about the model, please refer to Appendix A. On the other side, the spikes (deviating eigenvalues) of the spectrum map the event signals. They represent dominant information for system operating status.

B. Data Processing

Massive raw data can be represented by matrix naturally [24]. In a power system, assume that there are n kinds of measurable variables. At sampling time t_0 , we arrange the measured data of these variables in the form of a column vector $\hat{\mathbf{x}}(t_0) = (\hat{x}_{t_0,1}, \hat{x}_{t_0,2}, \dots, \hat{x}_{t_0,n})^H$ [25]. Then, arranging the column vectors $\hat{\mathbf{x}}(t_i)$ in chronological order ($i = 1, 2, \dots$), we obtain raw data source Ω .

For the raw data source Ω , we can cut off any arbitrary part, e.g., size of $N \times T$, at any time, e.g., sampling time t_i , forming $\tilde{\mathbf{X}}_{t_i} \in \mathbb{C}^{N \times T}$ as

$$\tilde{\mathbf{X}}(t_i) = (\hat{\mathbf{x}}(t_{i-T+1}), \hat{\mathbf{x}}(t_{i-T+2}), \dots, \hat{\mathbf{x}}(t_i)) \quad (2)$$

where $\hat{\mathbf{x}}(t_j) = (\hat{x}_{t_j,1}, \hat{x}_{t_j,2}, \dots, \hat{x}_{t_j,N})^H$ is measured data at sampling time t_j ($j = 1, 2, \dots, T$). It is worth noting that

T is the length of the moving split-window. If we keep the last sampling time as the current time, with the moving split-window, the real-time analytics is conducted.

Then, we convert the raw data matrix $\tilde{\mathbf{X}}_{t_i}$ obtained at each sampling time t_i into a standard non-Hermitian matrix $\tilde{\mathbf{X}}_{t_i}$ with the following algorithm.

$$\tilde{x}_{i,j} = (\hat{x}_{i,j} - \mu(\hat{\mathbf{x}}_i)) \times \frac{\sigma(\tilde{\mathbf{x}}_i)}{\sigma(\hat{\mathbf{x}}_i)} + \mu(\tilde{\mathbf{x}}_i) \quad (3)$$

where $\hat{\mathbf{x}}_i = (\hat{x}_{i,1}, \hat{x}_{i,2}, \dots, \hat{x}_{i,T})$, $\mu(\tilde{\mathbf{x}}_i) = 0$, $\sigma(\tilde{\mathbf{x}}_i) = 1$, $i = 1, 2, \dots, N$ and $j = 1, 2, \dots, T$.

In the following section, $\tilde{\mathbf{X}}_{t_i}$ is used to analyze the factors and noises at sampling time t_i .

III. FACTOR MODEL ALGORITHM

For a certain window, e.g. the one obtained at sampling time t_i , we aim to decompose the standard non-Hermitian matrix $\tilde{\mathbf{X}}_{t_i}$, as given in (3), into factors and residuals as follows:

$$\tilde{\mathbf{X}}_{t_i} = \mathbf{L}_{t_i,j} \mathbf{F}_{t_i,j} + \mathbf{U}_{t_i} \quad (4)$$

where p is the number of factors, $\mathbf{F}_{t_i,j}$ is the j -th factor, $\mathbf{L}_{t_i,j}$ is the corresponding loading, \mathbf{U}_{t_i} is the residual. Usually, only $\tilde{\mathbf{X}}_{t_i}$ is available, while $\mathbf{L}_{t_i,j}$, $\mathbf{F}_{t_i,j}$ and \mathbf{U}_{t_i} need to be estimated.

Factor model aims to simultaneously provide estimators of factor number and correlation structures in residuals. We turn the parameter-estimation problem into a minimum-distance problem. Specifically, we consider a minimum distance between the experimental spectral distribution $\rho_{\text{real}}(p)$ and the theoretical spectral distribution $\rho_{\text{model}}(b)$. The experimental one $\rho_{\text{real}}(p)$, depending on the sampling data, is obtained as empirical eigenvalue density (EED) of $\mathbf{C}_{\text{real}}^{(p)}$ in (7), and the theoretical one $\rho_{\text{model}}(b)$, based on Sokhotskys formula, is given as $\rho_{\text{model}}(\lambda; b)$ in (8). As a result, we turn the factor model estimation into a classical optimization as

$$\{\hat{p}, \hat{\theta}\} = \arg \min D(\rho_{\text{real}}(p), \rho_{\text{model}}(\theta)) \quad (5)$$

where D is a spectral distance measure or loss function. The solution of this minimization problem gives the number of factors, in the form of \hat{p} , and the parameters for the correlation structure of the residuals, in the form of $\hat{\theta}$.

A. Principal Component Estimation : $\rho_{\text{real}}(p)$

The first step is to generate p -level empirical residuals, by subtracting p largest principal components according to (4).

$$\hat{\mathbf{U}}^{(p)} = \tilde{\mathbf{X}}_{t_i} - \hat{\mathbf{L}}^{(p)} \hat{\mathbf{F}}^{(p)} \quad (6)$$

where $\hat{\mathbf{F}}^{(p)}$ is a $p \times T$ matrix of p factors, each row of which is a j -th ($j = 1, \dots, p$) principal component from $\tilde{\mathbf{X}}_{t_i}^T \tilde{\mathbf{X}}_{t_i}$, $\hat{\mathbf{L}}^{(p)}$ is an $N \times p$ matrix of factor loadings, estimated by multivariate least squares regression of $\tilde{\mathbf{X}}_{t_i}$ on $\hat{\mathbf{F}}^{(p)}$.

Then the covariance matrix from p -level residuals is obtained as

$$\mathbf{C}_{\text{real}}^{(p)} = \frac{1}{T} \hat{\mathbf{U}}^{(p)} \hat{\mathbf{U}}^{(p)T} \quad (7)$$

The subscript "real" indicates that $\mathbf{C}_{\text{real}}^{(p)}$ is obtained from real data. The steps can be summarized as follows:

Steps of Calculating $\rho_{\text{real}}(p)$

1. Calculate $\hat{\mathbf{F}}^{(p)}$: each row of which is a j -th principal component from correlation matrix of $\tilde{\mathbf{X}}_{ti}$, i.e. $\tilde{\mathbf{X}}_{ti}^T \tilde{\mathbf{X}}_{ti}$; denote as: $\hat{\mathbf{F}}^{(p)} = (f_1, f_2, \dots, f_p)^T$.
 2. Conduct least squares regression of $\tilde{\mathbf{U}}_{ti}$ on $\hat{\mathbf{F}}^{(p)}$: $\hat{\mathbf{L}}^{(p)} = \tilde{\mathbf{X}}_{ti} \hat{\mathbf{F}}^{(p)T}$.
 3. Calculate p -level residual: $\hat{\mathbf{U}}^{(p)} = \tilde{\mathbf{X}}_{ti} - \hat{\mathbf{L}}^{(p)} \hat{\mathbf{F}}^{(p)}$.
 4. Calculate covariance matrix from p -level residual:
 $\mathbf{C}_{\text{real}}^{(p)} = \frac{1}{T} \hat{\mathbf{U}}^{(p)} \hat{\mathbf{U}}^{(p)T}$.
 5. Calculate the empirical eigenvalue density of $\mathbf{C}_{\text{real}}^{(p)}$.
-

B. Modeling Covariance of Residuals: $\rho_{\text{model}}(\theta)$

In section II, we consider residuals as time series, which is represented by (1). The $\rho_{\text{model}}(\theta)$, however, is difficult to be obtained, since the limiting distribution of general A_N and B_T cost too much calculation resource via Stieltjes transform in [23]. Fortunately, a recent work by [26] provides an analytic derivation of limiting spectral density using free random variable techniques. This paper uses the results of [26] to calculate $\rho_{\text{model}}(\bullet)$. If we assume that the cross-correlations [23], i.e. \mathbf{A}_N , are effectively removed by the factors, then, the cross-correlations among the normalized residuals are negligible: $\mathbf{A}_N \approx \mathbf{I}_{N \times N}$. Under this assumption, only the auto-correlations, i.e. \mathbf{B}_T , left. The \mathbf{B}_T is in the forms of exponential decays with respect to time lags, as: $(\mathbf{B}_T)_{i,j} = b^{|i-j|}$. As a result, the $\rho_{\text{model}}(\theta_{A_N}, \theta_{B_T})$ is replaced by $\rho_{\text{model}}(b)$.

This enables us to calculate the modeled spectral density, $\rho_{\text{model}}(b)$, much more easily. It can be done through the free random variable techniques proposed in [26] (Refer to Appendix A for analytic derivation). The steps can be summarized as follows:

Steps of Calculating $\rho_{\text{model}}(b)$

1. Get the mean spectral density from Green Function $G(z)$ by using Sokhotskys formula:

$$\rho_{\text{model}}(\lambda; b) = -\frac{1}{\pi} \lim_{\varepsilon \rightarrow 0^+} \text{Im} G_c(\lambda + i\varepsilon) \quad (8)$$

2. Green Function $G(z)$ can be obtained from the Moments Generating Function $M(z)$

$$M(z) = zG(z) - 1 \quad (9)$$

3. Solve the polynomial equation for $M = M(z)$ ($a = \sqrt{1-b^2}$) and $c = N/T$ (a 6th-order polynomial equations for $\rho_{\text{model}}(\theta_{A_N}, \theta_{B_T})$):

$$a^4 c^2 M^4 + 2a^2 c (-(1+b^2)z + a^2 c) M^3 + ((1-b^2)^2 z^2 - 2a^2 c (1+b^2)z + (c^2 - 1)a^4) M^2 - 2a^4 M - a^4 = 0 \quad (10)$$

With the above procedure, we can rewrite (5) as

$$\{\hat{p}, \hat{b}\} = \arg \min D(\rho_{\text{real}}(p), \rho_{\text{model}}(b)) \quad (11)$$

C. Distance Measure

Since the empirical spectrum contains spikes, a distance measure which is sensitive to the presence of spikes should

be given. This paper uses Jensen-Shannon divergence, which is a symmetrized version of Kullback-Leibler divergence.

$$D_{\text{JS}}(P \| Q) = \frac{1}{2} D_{\text{KL}}(P \| M) + \frac{1}{2} D_{\text{KL}}(Q \| M) \quad (12)$$

where P and Q are probability densities, $M = \frac{1}{2}(P + Q)$, and $D_{\text{KL}}(P \| Q)$ is the Kullback-Leibler divergence defined by $D_{\text{KL}}(P \| Q) = \sum_i P_i \log \frac{P_i}{Q_i}$. Note that the Kullback-Leibler distance becomes larger if one density has a spike at a point while the other is almost zero at the same point. Refer to Appendix B for more details.

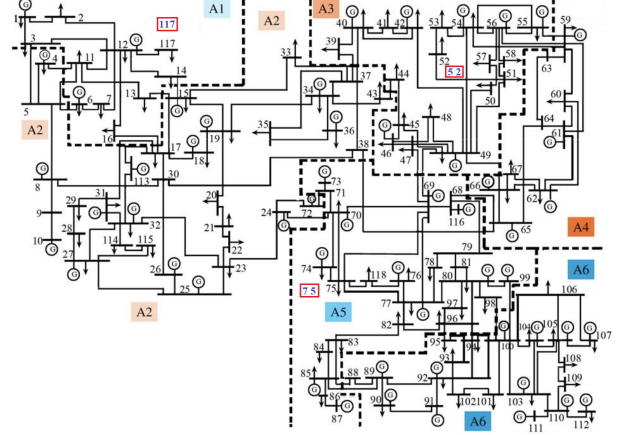


Fig. 1: Topology of the Standard IEEE 118-bus System.

IV. CASE STUDIES

The proposed method is tested with simulated data in the standard IEEE 118-bus system (the topology is shown in Fig. 1 on the Matpower platform [27]). In this simulations, we regard a sudden power consumption (active power, P) change on some node as an event.

Three cases are designed to validate the proposed method. In case 1, case 2, case 3, we set different numbers of events on node 52, 117, 75, and observe the number of factors, respectively. To make a comparison, we illustrate the results of the three cases in the same picture as Fig. 2.

The raw data source, Ω , is in size of $n=118$, $t=2500$. The size of the moving split-window is set to be $N=118$, $T=250$, i.e. $\hat{\mathbf{X}} \in \mathbb{C}^{118 \times 250}$.

Then, (11) is used to estimate the parameters p and b as \hat{p} and \hat{b} . The p for the number of the assumed events, and the b for the correlation structure of the noises. It is noted that we implement the simulated system model for dozens of times to collect data, the noise of each time follows the same distribution. The dozens times simulation is reasonable, as that we can obtain dozens observations for a real physical system through its sampling data, which have noises following a certain distribution.

Then, in the k -th simulation, Ω_k is generated. With (11), the estimation result \hat{p}_k and \hat{b}_k are obtained. For these \hat{p}_k and \hat{b}_k ($k = 1, 2, \dots$), their mean value \hat{p}_{ave} and \hat{b}_{ave} is calculated,

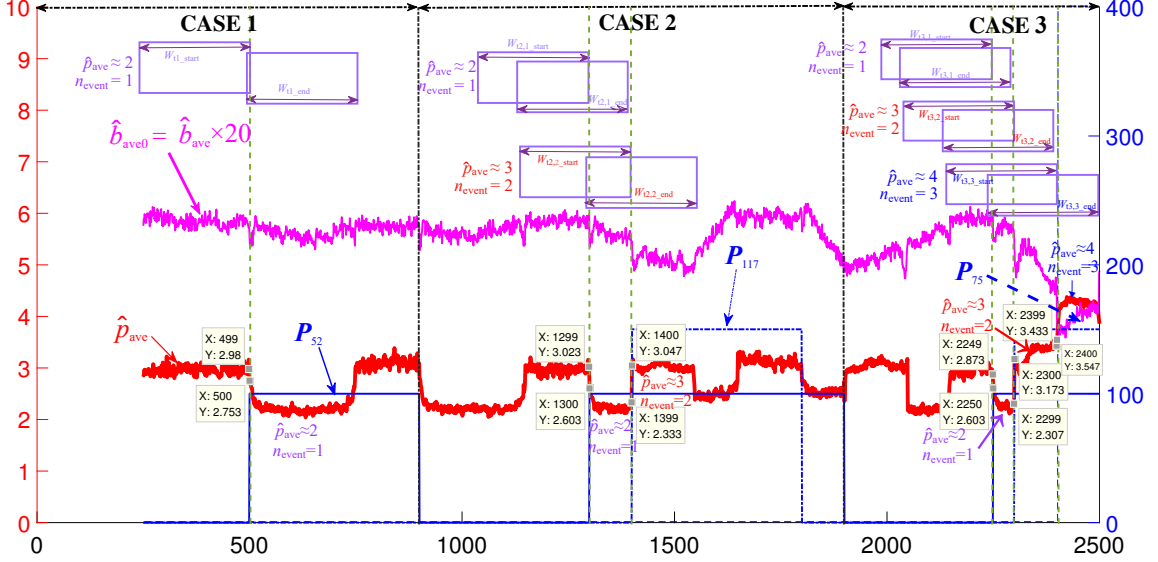


Fig. 2: Case Studies: (a) Case 1 (b) Case 2 (c) in Case 3.

which may appear in decimal form. We need to point out that the estimation of \hat{p}_{ave} and \hat{b}_{ave} begins at $t_s=250$ due to the length of the split-window. In Fig.2, we amplify the value of \hat{b}_{ave} for twenty times to make it obvious, i.e. $\hat{b}_{ave0} = \hat{b}_{ave} \times 20$.

The events in Case 1, Case 2, and Case 3 are given as Tab.II, Tab.III, and Tab.IV, respectively. The corresponding estimation results, i.e., the number of factors (i.e., \hat{p}_{ave}) and the correlation structure of the residuals (i.e., \hat{b}_{ave0}), are obtained as Fig. 2.

A. Case 1: Single Event Detection

Single Step Signal on Node 52:

TABLE II: Events Assumed in Case 1

Node	Sampling Time	Power Consumption P (MW)
52	$t_s = 1 \sim 499$ $t_s = 500 \sim 899$	$0+r_{52,t}$ $100+r_{52,t}$
others	$t_s = 1 \sim 899$	$c_k + r_{k,t}$

* c_k is a constant of node k , $k = \{1, 2, \dots, 118\} - \{52\}$.

* $r_{52,t}$, $r_{k,t}$ are noises following AR(1) model, where $b_{noise} = 0.5$.

Fig. 2(a) shows that:

- During the sampling time $t_s = 250 \sim 499$ ¹. \hat{p}_{ave} and \hat{b}_{ave} remain steady around 3 and 0.28, respectively.
- At $t_s=500$, \hat{p}_{ave} starts to decline to around 2. Also, \hat{b}_{ave} declines slightly.

Actually, as can be seen from Tab. II: no event occurs in the system when \hat{p}_{ave} keeps steady. Right at $t_s=500$, the P_{52} changes from 0 to 100MW. Therefore, we can conduct event detection with the proposed method.

Moreover, in this case, for the split-window $W_{t1} : t \in [251, 500]$, there exist a single-event (i.e., step signal on Node

52, s_{52} , at $t_s=500$) and 2 factors, i.e., 1 event, $\hat{p}_{ave} \approx 2$ during $W_{t1,Start} : t \in [251, 500]$ to $W_{t1,End} : t \in [650, 899]$. A linear relationship between the number of events and the number of factors will be revealed afterwards.

B. Case 2: Multiple Event Detection (Two Events)

Multiple Step Signal on Node 52 and Node 117:

TABLE III: Events Assumed in Case 2

Node	Sampling Time	Active Load (MW)
52	$t_s = 900 \sim 1299$ $t_s = 1300 \sim 1899$	$0+r_{52,t}$ $100+r_{52,t}$
117	$t_s = 900 \sim 1399$ $t_s = 1400 \sim 1799$ $t_s = 1800 \sim 1899$	$0+r_{117,t}$ $150+r_{117,t}$ $0+r_{117,t}$
others	$t_s = 900 \sim 1899$	$c_k + r_{k,t}$

Fig. 2(b) shows that:

- During the sampling time $t_s = 1149 \sim 1299$ ², \hat{p}_{ave} and \hat{b}_{ave} remain steady. Thus, we deduce that no event occurs in the system, which meets Tab. III.
- At $t_s=1300$, \hat{p}_{ave} starts to decline (from 3.023 to 2.603) and then keeps around 2 till $t_s=1399$. For the split-window $W_{t2,1,Start} : t \in [1051, 1300]$ to $W_{t2,1,End} : t \in [1150, 1399]$, there exist a single-event (i.e., s_{52} at $t_s=1300$) and 2 factors, i.e., 1 event, $\hat{p}_{ave} \approx 2$.
- At $t_s=1400$, \hat{p}_{ave} starts to raise (from 2.333 to 3.047) and then keeps around 3. For the split-window $W_{t2,2,Start} : t \in [1151, 1400]$ to $W_{t2,2,End} : t \in [1299, 1548]$, there exist two multi-event (i.e., s_{52} at $t_s=1300$, s_{117} at $t_s=1400$) and 3 factors, i.e., 2 event, $\hat{p}_{ave} \approx 3$.

¹250 = 1(The beginning of Signal)+250(Length of Split-Window)-1

²1149 = 900(The beginning of Signal)+250(Length of Split-Window)-1

C. Case 3: Multiple Event Detection (Three Events)
Multiple Step Signal on Node 52, Node 117 and Node 75:

TABLE IV: Events Assumed in Case 3

Node	Sampling Time	Active Load (MW)
52	$t_s = 1900 \sim 2249$	$0+r_{52,t}$
	$t_s = 2250 \sim 2500$	$100+r_{52,t}$
117	$t_s = 1900 \sim 2299$	$0+r_{117,t}$
	$t_s = 2300 \sim 2500$	$150+r_{117,t}$
75	$t_s = 1900 \sim 2399$	$0+r_{75,t}$
	$t_s = 2400 \sim 2500$	$400+r_{75,t}$
others	$t_s = 1900 \sim 2500$	$c_k + r_{k,t}$

Fig. 2(c) shows that:

- During the sampling time $t_s = 2149 \sim 2249^3$, \hat{p}_{ave} and \hat{b}_{ave} remain steady. Thus, we deduce that no event occurs in the system, which meets Tab. IV.
- At $t_s=2250$, \hat{p}_{ave} starts to decline (from 2.873 to 2.603) and then keeps around 2 till $t_s=2300$. For the split-window $W_{t3,1Start} : t \in [2001, 2250]$ to $W_{t3,1End} : t \in [2050, 2299]$, there exist a single-event (i.e., s_{52} at $t_s=2250$) and 2 factors, i.e., 1 event, $\hat{p}_{ave} \approx 2$.
- At $t_s=2300$, \hat{p}_{ave} starts to raise (from 2.307 to 3.173) and then keeps around 3 till $t_s=2400$. For the split-window $W_{t3,2Start} : t \in [2051, 2300]$ to $W_{t3,2End} : t \in [2150, 2399]$, there exist two multi-event (i.e., s_{52} at $t_s=2250$, s_{117} at $t_s=2300$) and 3 factors, i.e., 2 event, $\hat{p}_{ave} \approx 3$.
- At $t_s=2400$, \hat{p}_{ave} starts to raise (from 3.433 to 3.547) and then keeps around 4. For the split-window $W_{t3,3Start} : t \in [2151, 2400]$ to $W_{t3,3End} : t \in [2251, 2500]$, there exist three multi-event (i.e., s_{52} at $t_s=2250$, s_{117} at $t_s=2300$, s_{75} at $t_s=2400$) and 4 factors, i.e., 3 event, $\hat{p}_{ave} \approx 4$.

D. Further Discussions about the Cases

Through the above three cases, the relationship between the number of events (i.e., n_{event}) and the number of factors (i.e., \hat{p}_{ave}) is revealed.

The results of the three cases are summarized in Tab. V:

TABLE V: Relationship between Event Number (n_{event}) and Factor Number (\hat{p}_{ave})

Case	Split Window	n_{event}	\hat{p}_{ave}
1	[251, 500] ~ [650, 899]	1	2
2	[1051, 1300] ~ [1150, 1399]	1	2
	[1151, 1400] ~ [1299, 1548]	2	3
3	[2001, 2250] ~ [2050, 2299]	1	2
	[2051, 2300] ~ [2150, 2399]	2	3
	[2151, 2400] ~ [2251, 2500]	3	4

\hat{p}_{ave} , estimated by factor model, is approximately equal to n_{event} plus one, i.e. $\hat{p}_{ave} \approx n_{event} + 1$. There exists a linear relationship between them. Therefore, we can deduce the number of the multi-event for a certain split-window.

³2149 = 1900(The beginning of Sigal)+250(Length of Split-Window)−1

Besides, every time an event occurs, \hat{b}_{ave} drops. It indicates that the correlation in the residuals decreases when there exit events.

V. CONCLUSION

This paper proposes a data-driven method, namely, factor model, to conduct multi-event detection and recognition in a large power system. In the analysis procedure, we estimate the number of factors p and the parameter for the correlation structure of residuals b by minimizing the distance between two spectrums. Then, we conduct real-time analysis of the two parameters, p and b , using moving split-window. The proposed method is direct and practical for multi-event analytics in a complex situation. Following conclusions are obtained: First, the number of factors estimated by factor model has an approximately linear relationship with the number of events that occur in the system. Second, taking non-Gaussian noises into account, time series analytics is implemented to extract the information from noises. The decrease of parameter b is related to the occurrence of events. It is noted that, the number of factors reveal the spatial information (events on different nodes) in the system; while the correlation structure in noises contains temporal information. The proposed method considers space-time correlation in a large power system. Finally, case studies verify the effectiveness of the method.

Along this direction, following work can be done. For example, we can employ more general modeling for noises. If we consider vector ARMA (1, 1) processes, we have up to 6th-order polynomial equations [26]. Furthermore, the relationship between the number of factors and events can be further studied with physical model.

APPENDIX A

AN OVERVIEW OF FREE RANDOM VARIABLE TECHNIQUES

We summarize the main concepts and key results in free random variables techniques that we employ to derive $\rho_{mod\ el}(b)$. We follow the notations and derivations from [26, 28]. First, consider a simple decomposition of covariance structures:

$$Cov_{ia,jb} = A_{ij}B_{ab} \quad (13)$$

where A is an $N \times N$ cross-covariance matrix and B is a $T \times T$ auto-covariance matrix, $i, j = 1 \cdots N$, $a, b = 1 \cdots T$. Suppose G is an $N \times T$ *i.i.d* Gaussian random matrix. Then a correlated Gaussian random matrix U ($N \times T$ time series) can be written as $U = A_N^{1/2}GB_T^{1/2}$. Its sample (empirical) covariance matrix C is

$$C = \frac{1}{T}UU^T = \frac{1}{T}A^{1/2}GBG^T A^{1/2} \quad (14)$$

Consider a real symmetric $N \times N$ random matrix H .

Definition 1 Mean Spectral Density

$$\rho_H(\lambda) = \frac{1}{N} \sum_{i=1}^N \langle \delta(\lambda - \lambda_i) \rangle = \frac{1}{N} \langle Tr(\lambda 1_N - H) \rangle \quad (15)$$

where the expectation $\langle \cdots \rangle$ is taken w.r.t. the rotationally invariant probability measure, $\delta(\bullet)$ is a Dirac delta function,

and 1_N is a $N \times N$ unit matrix.

Definition 2 The Greens Function (or Stieltjes Transform)

$$\begin{aligned} G_H(z) &= \frac{1}{N} \sum_{i=1}^N \left\langle \frac{1}{z - \lambda_i} \right\rangle = \frac{1}{N} \left\langle \frac{1}{z 1_N - H} \right\rangle \\ &= \int \frac{\rho_H(\lambda)}{z - \lambda} d\lambda \end{aligned} \quad (16)$$

The relationship between $\rho_H(\lambda)$ and $G_H(z)$ is:

$$\rho_H(\lambda) = -\frac{1}{\pi} \lim_{\varepsilon \rightarrow 0^+} \text{Im} G_H(\lambda + i\varepsilon) \quad (17)$$

The Greens function generates moments of a probability distribution, where the n -th moment is defined by:

Definition 3 Moment

$$m_n = \frac{1}{N} \langle \text{Tr} H^n \rangle = \int \rho_H(\lambda) \lambda^n d\lambda \quad (18)$$

Definition 4 Moment Generating Function

$$\begin{aligned} G_H(z) &= \sum_{n \geq 0} \frac{m_n}{z^{n+1}} \\ M_H(z) &= \sum_{n \geq 1} \frac{m_n}{z^{n+1}} \end{aligned} \quad (19)$$

The relationship between $G_H(z)$ and $M_H(z)$ is

$$M_H(z) = zG_H(z) - 1 \quad (20)$$

Blues function and N-transform are the inverse transform of the Greens function and moment generating function, respectively.

Definition 5 Blues function and N-transform

$$\begin{aligned} G_H(B_H(z)) &= B_H(G_H(z)) = z \\ M_H(N_H(z)) &= N_H(M_H(z)) = z \end{aligned} \quad (21)$$

Then, return to Eq.13. The N-transform of C can be derived as:

$$N_C(z) = rzN_B(rz)N_A(z) \quad (22)$$

Using the moments generating function $M \equiv M_C(z)$ and its inverse relation to N-transform, Eq.20 can be written as:

$$z = rMN_B(rM)N_A(M) \quad (23)$$

Now, we consider the simplified model with $A_N \approx I_{N \times N}$. In such case, U_{nt} is a time-series (AR(1)) following the autoregressive model:

$$U_{nt} = bU_{n,t-1} + \xi_{nt} \quad (24)$$

where $|b| < 1$, $\xi_{nt} \sim N(0, 1 - b^2)$, $n = 1, \dots, N$, $t = 1, \dots, T$. We calculate the eigenvalue distribution $\rho_C(\lambda)$ of correlation matrix $C = \frac{1}{T}UU^T$ based on the following strategy.

Step 1: Find $M_C(z)$, from the equation for N-transform.

Step 2: Find $G_C(z)$, by Eq.19.

Step 3: Find $\rho_C(\lambda)$, by Eq.16.

For *Step 1*, consider Eq.22. Because $A_N \approx I_{N \times N}$, so $N_A(z) = 1 + 1/z$. Therefore, Eq.22 can be rewritten as:

$$\frac{z}{r(1+M)} = N_B(rM)$$

$$rM = M_B\left(\frac{z}{r(1+M)}\right) \quad (25)$$

To find M_B , note that the auto-covariance matrix of AR(1) process has a simple form:

$$B_{st} = \frac{\text{var}(\zeta)}{1 - b^2} b^{|s-t|} = b^{|s-t|} \quad (26)$$

Using Fourier-transform of the matrix B , it can be shown that the moment generating function of B is

$$M_B(z) = -\frac{1}{\sqrt{1-z} \sqrt{1 - \frac{(1+b^2)^2}{1-b^2} z}} \quad (27)$$

Therefore, we obtain Eq.10 for *Step 1*. The other steps are followed straightforwardly as Eq.9 and Eq.8.

APPENDIX B

KULLBACK-LEIBLER DIVERGENCE

The Kullback-Leibler divergence is defined as follows:

$$D_{KL}(P \| Q) = \sum_i P_i \log \frac{P_i}{Q_i} \quad (28)$$

where P and Q are probability densities. To deal with zero elements of P , we use:

$$\tilde{P}_i = \begin{cases} \alpha P_i & , P_i > 0 \\ \varepsilon & , P_i = 0 \end{cases} \quad (29)$$

where ε is a small enough positive number. Denote the number of zero elements in P as num , $\alpha = 1 - num \times \varepsilon$. Probability density Q is dealt with in the same way.

REFERENCES

- [1] X. Xu, X. He, Q. Ai, and R. C. Qiu, "A correlation analysis method for power systems based on random matrix theory," *IEEE Transactions on Smart Grid*, vol. PP, no. 99, pp. 1–10, 2015.
- [2] X. Miao and D. Zhang, "The opportunity and challenge of big data's application in distribution grids," in *China International Conference on Electricity Distribution*, 2014, pp. 962–964.
- [3] J. Zhang and M. L. Huang, "5ws model for big data analysis and visualization," in *IEEE International Conference on Computational Science and Engineering*, 2013, pp. 1021–1028.
- [4] M. Mayilvaganan and M. Sabitha, *A cloud-based architecture for Big-Data analytics in smart grid: A proposal*, 2013.
- [5] X. He, Q. Ai, R. C. Qiu, W. Huang, L. Piao, and H. Liu, "A big data architecture design for smart grids based on random matrix theory," *IEEE Transactions on Smart Grid*, vol. 8, no. 2, pp. 674–686, 2017.
- [6] X. He, R. C. Qiu, Q. Ai, and X. Xu, "An unsupervised learning method for early event detection in smart grid with big data," *Computer Science*, 2015.
- [7] L. Chu, R. C. Qiu, X. He, Z. Ling, and Y. Liu, "Massive streaming pmu data modeling and analytics in smart grid

- state evaluation based on multiple high-dimensional covariance tests,” IEEE Transactions on Big Data, vol. PP, no. 99, pp. 1–1, 2016.
- [8] M. J. Smith and K. Wedeward, “Event detection and location in electric power systems using constrained optimization,” in IEEE Power and Energy Society General Meeting, 2009, pp. 1–6.
- [9] S. Soltan, D. Mazauric, and G. Zussman, “Cascading failures in power grids: analysis and algorithms,” in International Conference on Future Energy Systems, 2014, pp. 195–206.
- [10] M. He and J. Zhang, “A dependency graph approach for fault detection and localization towards secure smart grid,” IEEE Transactions on Smart Grid, vol. 2, no. 2, pp. 342–351, 2011.
- [11] L. Xie, Y. Chen, and P. R. Kumar, “Dimensionality reduction of synchrophasor data for early event detection: Linearized analysis,” IEEE Transactions on Power Systems, vol. 29, no. 6, pp. 2784–2794, 2014.
- [12] M. Rafferty, X. Liu, D. M. Lavery, and S. Mcloone, “Real-time multiple event detection and classification using moving window pca,” IEEE Transactions on Smart Grid, vol. 7, no. 5, pp. 2537–2548, 2016.
- [13] Y. Wang, M. Liu, and Z. Bao, “Deep learning neural network for power system fault diagnosis,” in Control Conference, 2016, pp. 6678–6683.
- [14] S. Naderian and A. Salemnia, “An implementation of type2 fuzzy kernel based support vector machine algorithm for power quality events classification,” International Transactions on Electrical Energy Systems, vol. 27, no. 5, pp. –, 2016.
- [15] M. Forni, A. Giovannelli, M. Lippi, and S. Soccorsi, “Dynamic factor model with infinite dimensional factor space: Forecasting,” Center for Economic Research, 2016.
- [16] J. Yeo and G. Papanicolaou, “Random matrix approach to estimation of high-dimensional factor models,” Papers, 2016.
- [17] Z. Sun, X. Liu, and L. Wang, “A hybrid segmentation method for multivariate time series based on the dynamic factor model,” Stochastic Environmental Research and Risk Assessment, pp. 1–14, 2016.
- [18] E. P. Wigner, “On a class of analytic functions from the quantum theory of collisions,” Annals of Mathematics, vol. 53, no. 1, pp. 36–67, 1951.
- [19] V. Plerou, P. Gopikrishnan, B. Rosenow, L. A. N. Amaral, and H. E. Stanley, “Universal and non-universal properties of cross-correlations in financial time series,” Papers, vol. 83, no. 7, pp. 1471–1474, 2012.
- [20] L. LALOUX, P. CIZEAU, M. POTTERS, and J.-P. BOUCHAUD, “Random matrix theory and financial correlations,” International Journal of Theoretical and Applied Finance, vol. 3, no. 03, pp. 391–397, 2000.
- [21] S. C. Chevalier and P. D. H. Hines, “Identifying system-wide early warning signs of instability in stochastic power systems,” in Power and Energy Society General Meeting, 2016, pp. 1–5.
- [22] C. Xu, J. Liang, Z. Yun, and L. Zhang, “The small-disturbance voltage stability analysis through adaptive ar model based on pmu,” in Transmission and Distribution Conference and Exhibition: Asia and Pacific, 2005 IEEE/PES, 2005, pp. 1–5.
- [23] L. Zhang, “Spectral analysis of large dimensional random matrices,” Ph D, 2007.
- [24] R. Qiu and M. Wicks, Cognitive Networked Sensing and Big Data. Springer Publishing Company, Incorporated, 2013.
- [25] D. L. Donoho, “High-dimensional data analysis: The curses and blessings of dimensionality,” 2000.
- [26] Z. Burda, A. Jarosz, M. A. Nowak, and M. Snarska, “A random matrix approach to varma processes,” vol. 12, no. 1002.0934, pp. 1653–1655, 2010.
- [27] R. D. Zimmerman and C. E. Murillo-Snchez, “Matpower 4.1 user’s manual,” Power Systems Engineering Research Center, 2011.
- [28] B. Z, J. J, and W. B, “Spectral moments of correlated wishart matrices.” Phys.rev.e, vol. 71, no. 2 Pt 2, p. 026111, 2005.